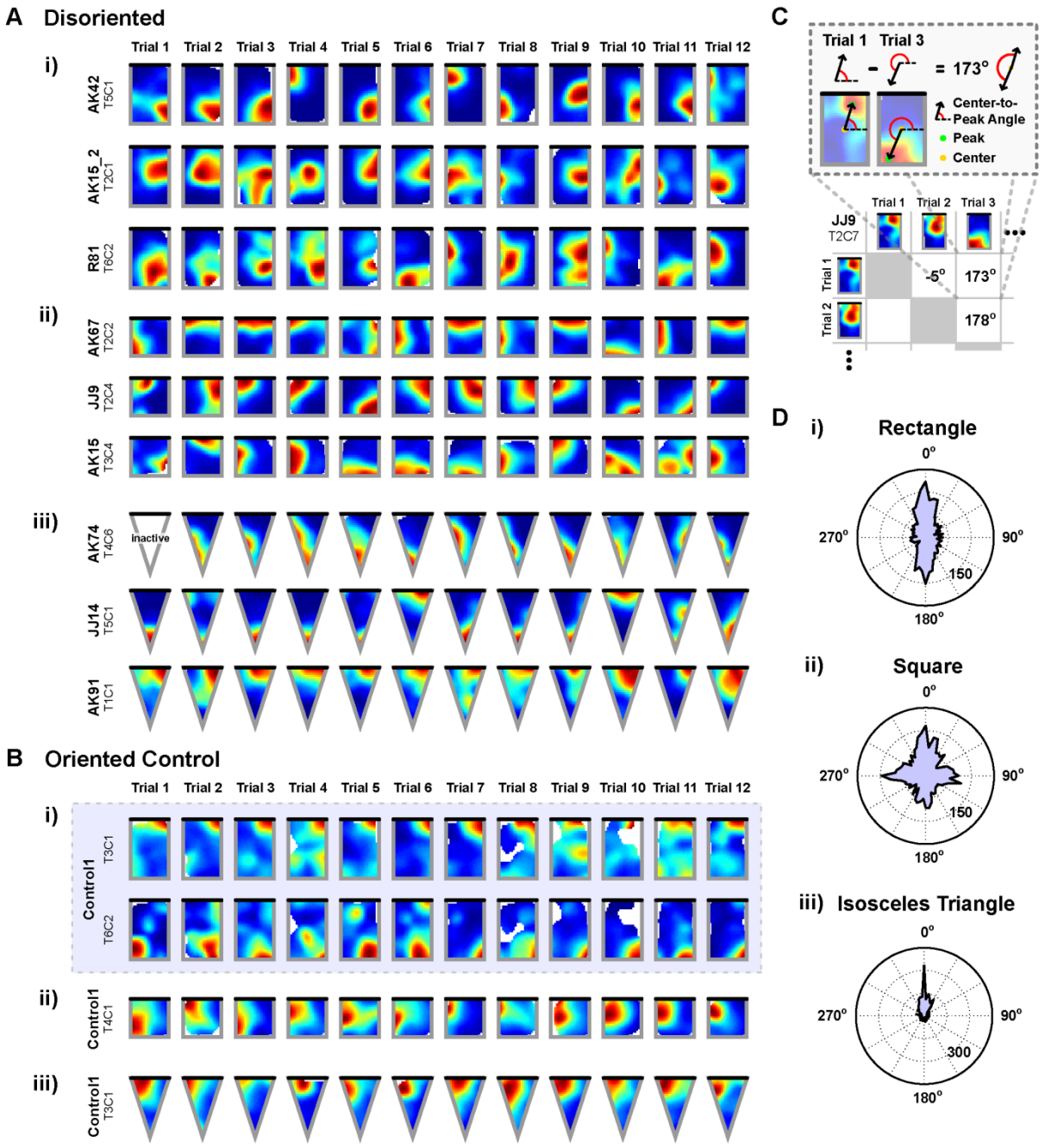

Figure S1. Supplemental results for the foraging experiments. Related to Figures 1 and 2.

Additional examples of place cell rate maps from A) 3 disoriented mice and B) one oriented control mouse for all 12 trials of foraging in: i) the rectangular, ii) the square, and iii) the isosceles triangular chambers. The black line on the edge of the chamber indicates the location of the nongeometric visual cue. C) Schematic of the center-to-peak angle analysis. First, for each cell and trial the angle from the center of the environment to the pixel with maximum firing was measured. Then for each pair of trials within each cell, the difference between the center-to-peak angles was computed. Finally, a histogram representing the distribution of these center-to-peak angles across all cells and pairwise trial comparisons was created. Note that this analysis does not rely on compression of rate maps. D) Polar histograms resulting from the center-to-peak angle analysis of disoriented mice in: i) the rectangular, ii) the square, and iii) the isosceles triangular chambers during foraging. Radius indicated in the lower right of each histogram. Note that the maxima of these distributions mirror the rotational symmetry of each chamber.

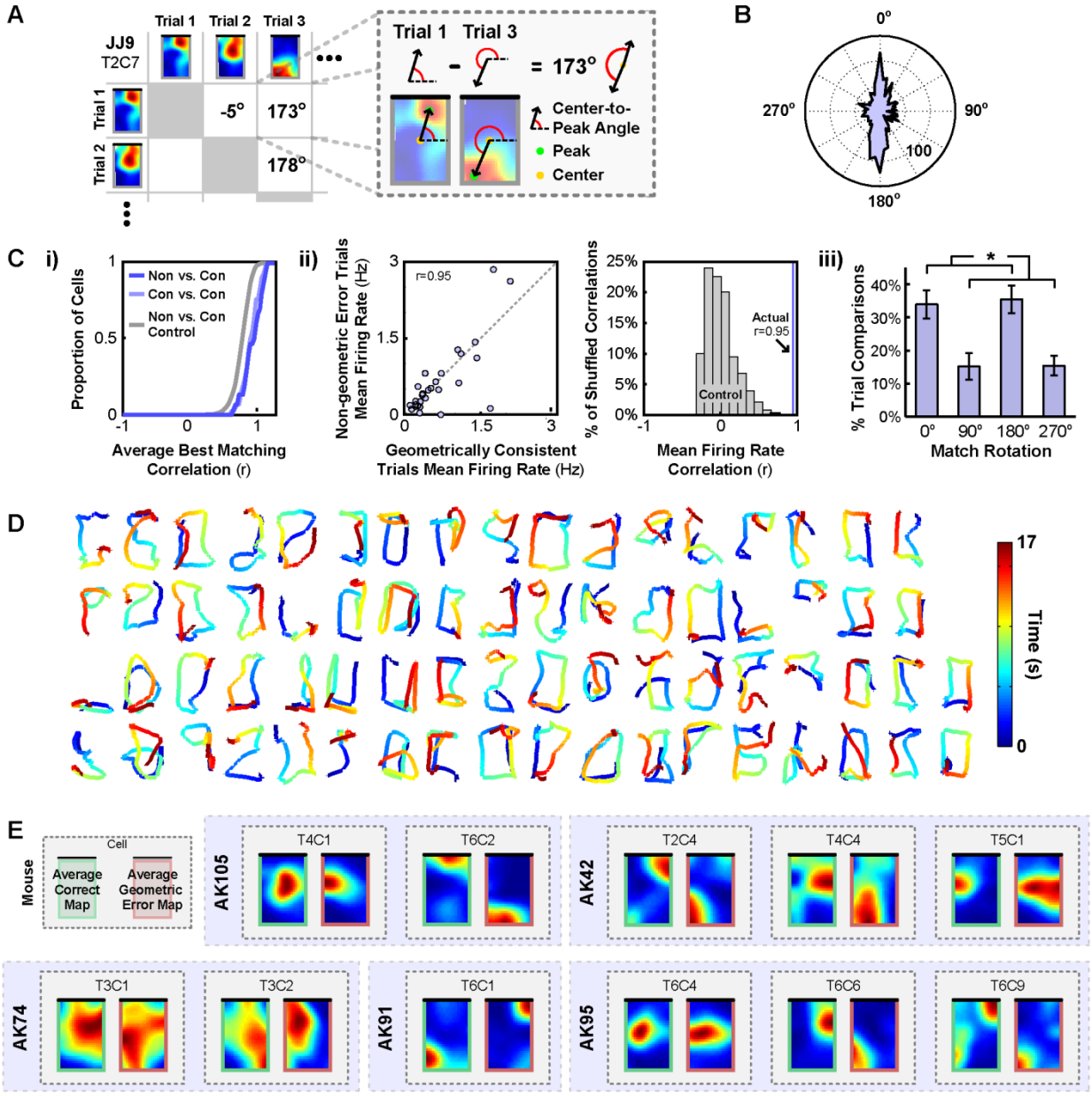

Figure S2. Supplemental results for the spatial reorientation task experiment. Related to Figure 3.

A)Schematic of the center-to-peak angle analysis as in Figure S1c. First, for each cell and trial the angle from the center of the environment to the pixel with maximum firing was measured. Then for each pair of trials within each cell, the difference between the center-to-peak angles was computed. Finally, a histogram representing the distribution of these center-to-peak angles across all cells and pairwise trial comparisons was created. Note that this analysis does not rely on compression of rate maps.

B) Polar histograms resulting from the center-to-peak angle analysis in the rectangular chamber during the spatial reorientation task. Radius indicated in the lower right of the histogram. Note that the maxima of this distribution mirror the rotational symmetry of the chamber.

C) Although nongeometric searches (searches at locations other than the correct and geometric error locations) were rare, all but one mouse made at least one nongeometric error (4 mice made 1 nongeometric error, 2 mice made 2

nongeometric errors). We assessed the potential hippocampal contribution to nongeometric error trials by comparing the hippocampal maps between nongeometric error and geometrically consistent search trials in three different ways:

i) To assess whether place cells exhibited similar maps on geometrically consistent (Con) and nongeometric error (Non) trials, we first computed the similarity between geometrically consistent and nongeometric error rate maps. The average best match correlation values for comparisons between geometrically consistent and nongeometric error trial rate maps was high (Non vs. Con; $r=0.728\pm0.024$), exceeding the shuffled control ($p<0.001$; see Supplementary Methods below). Moreover, the similarity between geometrically consistent and nongeometric error trial rate maps was not different from the similarity between two geometrically consistent trial rate maps (Con vs. Con; $r=0.70\pm0.018$; paired t-test: $t(29)=0.68$, $p=0.50$). These results indicate that the preferred firing locations of place cells did not globally remap to new locations during nongeometric error trials.

ii) Given that the preferred firing locations of cells did not remap, we next asked whether rate differences might underlie nongeometric error trials. Mean firing rates during nongeometric error and geometrically consistent trials were highly correlated ($r=0.95$, $p<0.001$). This correlation exceeded its shuffled control generated by shuffling the nongeometric error trial mean firing rates across cells 1000 times ($p<0.001$). These results suggest that no reliable rate remapping was observed during nongeometric error trials.

iii) Because similar rate maps and firing rates were observed during nongeometric error and geometrically consistent search trials, we lastly asked whether 90° or 270° map rotations might underlie these nongeometric errors. To do so, we computed the percent of pairwise trial comparisons for which each rotation (0°, 90°, 180°, or 270°) yielded the best match, restricted to comparisons of nongeometric error trial rate maps to geometrically consistent trial rate maps. An initial repeated measures ANOVA indicated that not all rotations yielded the best match equally often ($F(1.6,8.1)=6.2$, $p=0.027$; Greenhouse-Geisser corrected). Rather, rotations by 0° or 180° yielded the best match more often than rotations by 90° or 270° (paired t-test: $t(5)=2.9$, $p=0.033$), and best match rotations of 0° and 180° rotations occurred with similar frequency (paired t-test: $t(5)=0.3$, $p=0.77$). These results indicate that nongeometric error searches were not linked to 90° or 270° rotations of the hippocampal map. Rather, the spatial geometry alone continued to orient hippocampal representations on nongeometric error trials. Therefore, the orientation of the hippocampal map did not dictate the behavior of the animal during error trials. Error bars denote mean ± 1 SEM. *$p<0.05$

The similarity of the rate maps, firing rates, and distribution of preferred orientations between geometrically consistent and nongeometric error searches suggests that nongeometric errors may be the product of extra-hippocampal circuits. Nevertheless, because nongeometric errors were very rare, we refrain from drawing strong conclusions about the mechanism underlying these errors.

D) Search paths during the first 17 s of each trial, at which point the hippocampal map is predictive of search behavior. Note that on most trials the animals spend the first seconds exploring the perimeter of the chamber.

E) Example average correct and average geometric error maps from all mice not shown in Figure 3. All analyzed trials during the spatial reorientation task are included in the average maps. Blue shading indicates simultaneously recorded cells. The black line on the edge of the chamber indicates the location of the nongeometric visual cue.

Supplemental Experimental Procedures

Subjects

Naive male mice 2-6 months of age (C57Bl/6, Jackson Laboratory, Bar Harbor, ME) were housed individually on a 12-hour light/dark cycle. To increase motivation to participate in all experiments, the mice were maintained at 85%-90% of their *ad libitum* weight. All experiments were carried out during the light portion of the light/dark cycle, and in accordance with NIH guidelines and approved by the Institution of Animal Care and Use Committee of the University of Pennsylvania and the University of Texas at San Antonio.

Experimental Protocol

Chambers. The rectangular chamber consisted of four white walls (short walls 20 cm x long walls 30 cm x height 35 cm), with three evenly-spaced 4 cm wide vertically-oriented black stripes spanning one short wall serving as the nongeometric visual cue. The square chamber consisted of four white walls (all walls 20 cm x height 35 cm), with three evenly-spaced 4 cm wide horizontally-oriented black stripes spanning one wall serving as the nongeometric visual cue. The isosceles triangular chamber consisted of two white walls (long walls 30 cm x height 35cm), with one solid black wall (short wall 20 cm x height 35 cm) serving as the nongeometric visual cue. Previous experiments have demonstrated that both oriented and disoriented mice can easily discriminate with these nongeometric visual cues [S1]. During all experiments, these chambers were surrounded by a large white cylinder (diameter 70 cm x height 70 cm) and a black curtain to eliminate distal visual cues.

Trial Protocol. Trial structure was similar for all experiments. Prior to each trial, the mouse was placed in a PVC cylinder (diameter 9 cm x height 30 cm) with a detachable base and lid for disorientation. The chamber was vacuumed, wiped down with ethanol to eliminate potential odor cues, and rotated 90° clockwise relative to the previous trial orientation to ensure that the hippocampal map did not track any external cues. To disorient the mouse, the experimenter rotated the cylinder on a turntable four full revolutions clockwise and then again counterclockwise (~180°/sec). The mouse was then immediately placed in the center of the chamber, and the base of the disorientation cylinder was removed so that the mouse stood on the floor of the chamber still encapsulated by the lidded disorientation cylinder. The disorientation cylinder was removed, and the mouse could freely move about the chamber. From the end of disorientation to release in the chamber took ~15 s. Once the trial criteria were met, the mouse was removed, placed back in the disorientation cylinder, and allowed to rest for ~2 min before the beginning of the next trial. A white noise generator was placed above the chamber throughout all experiments to mask any potential distal sound cues. Trial protocol was the same for the oriented control mouse, except that the mouse was never disoriented, held in their home cage between trials, and the chamber was not rotated between trials.

Foraging experiments. During foraging experiments, neural activity was recorded from right dorsal CA1 as disoriented mice (and one oriented control mouse) foraged for small amounts of a food reward (crushed up Kellogg's Cocoa Krispies) scattered throughout the entire chamber prior to the start of each trial. Mice completed one experimental session a day for up to three days, each of which consisted of 12 consecutive trials. Each session took place in one of the three chambers. During each trial, mice foraged for at least three minutes until the chamber was adequately sampled.

Spatial reorientation task experiment. Two days prior to the beginning of the recording, mice were shaped to dig for a food reward buried in a medicine cup placed in their home cage. Once hippocampal cells were identified and the quality of the clusters was checked (see below Electrophysiology), neural activity was recorded from the right dorsal CA1 area as disoriented mice completed a traditional spatial reorientation task. The task consisted of 12 trials per day (one mouse, EM1, received 8 trials per day) in the rectangular chamber containing four medicine cups embedded in the floor near each corner. All medicine cups were filled to the brim with scented bedding (cumin or ginger mixed with regular bedding). For any given animal, the same scent was used for all trials. The right cup nearest the nongeometric visual cue was consistently rewarded on each trial with the buried food reward. On each trial the mouse was disoriented and then released in the chamber to search for the buried reward. The cup in which the mouse first dug was recorded as the measure of search behavior. The mouse remained in the chamber for at least three minutes until the chamber was adequately sampled and the reward was retrieved. To shape learning, the reward was exposed on the first two trials of the first day. These trials were excluded from subsequent analysis. To ensure that search behavior reflected memory for the reward location and not simply random searching, this task

was repeated each day until a performance criterion was met. Specifically, for each mouse, data were analyzed only for the first day during which at least 66% of searches were at the correct or geometric error locations (range 1 to 3 days; Criteria was met on Day 1 for most mice, except AK74 (Day 2) and EM1 (Day 3)). This criteria was established prior to recording on the basis of pilot results from [S1], and all mice exceeded this criteria and achieved an accuracy of at least 75% on the analyzed day.

Order of experimental conditions. To maximize the amount of electrophysiological data collected, the majority of mice participated in multiple experimental conditions. The table below lists the order in which each mouse completed each experiment. There were no systematic increases or decreases in the stability of the hippocampal map within any animal across chambers or experiments. However, behavioral prediction accuracy in the spatial reorientation task may be related to prior experience with disorientation or environments, as prediction accuracy was highest among animals that did not experience any other experimental conditions. Nevertheless, we refrain from drawing strong conclusions about this relationship because of the limited number of animals run in each order.

	Foraging			Behavior
Mouse Name	Rectangle	Square	Triangle	Rectangle
AK8	1	2		
JJ9	1	2		
AK15	1	2	3	
AK15_2	1	2	3	
JJ14	1	2	3	
AK67	1	2	3	
AK42	1	2	3	4
R81	1	2	3	4
AK74	3	4	1	2
AK91			1	2
AK95				1
AK105				1
EM1				1
Control1	1	2	3	

Surgery

Mice were anesthetized with a mixture of ketamine (100 mg/kg) and xylazine (10 mg/kg) administered intraperitoneally (0.1 ml/kg) and placed flat on a stereotaxic frame (David Kopf Instruments). They were then implanted with drivable 6-tetrode microdrives above the right dorsal hippocampus (from Bregma (in mm): AP, -1.7; ML, -1.6; DV, -1.0). A ground wire was connected to a screw placed on the contralateral side of the skull above the occipital lobe. The headstages were affixed to the skulls with cyanoacrylate and dental cement.

Electrophysiology

Beginning one week after surgery, neural activity from each tetrode was screened daily. The search for cells was conducted in a circular chamber (diameter 35cm x height 35cm). The headstage was connected to a tethered unity gain amplifier with green and red LEDs for tracking the position of the mouse. Units were amplified using a 32-channel amplifier (Neuralynx), and electrical signals were amplified between 2,500 and 10,000 times and filtered between 400-9,000 Hz. The amplifier output was digitized at 30.3 kHz. The position of the mouse and electrophysiological data were recorded by Cheetah Data Acquisition software (Neuralynx). The tetrode bundle was slowly advanced by 15-20 μm steps per day into recording position, lowering the tetrodes in small steps to minimize electrode drift [S2,S3]. Pyramidal cells were identified by their characteristic firing patterns [S4]. After completion

of an experimental session, units were cluster cut and analyzed using MClust software (developed by A. David Redish, University of Minnesota). Cells were only accepted for analysis if they formed isolated Gaussian clusters with minimal overlap with surrounding cells and noise. Cells were cut simultaneously from all concatenated trials recorded on the same day, without knowledge of the trials from which they originated to eliminate any potential bias in spike sorting. No attempt was made to track the same cells across days. All further analyses were carried out offline in MATLAB using custom-written scripts.

Analyses

Inclusion criteria. Only data from periods of movement in which the velocity of the mouse exceed 2cm/s were included in the analysis. Only cells firing at least 15 spikes during periods of movement during a trial were included in the analysis of that trial.

Rate maps. Rate maps for each cell were created by first binning the chamber into 1 cm x 1 cm pixels, and counting the number of spikes and the amount of time the mouse spent in each pixels. Both the spike map and the time map were then smoothed with an isometric Gaussian kernel with a standard deviation of 3 cm. The final place field map was then the result of the smoothed spike map divided by the smoothed time map. Only pixels sampled for at least 0.05sec after smoothing were considered sampled.

Best match rotations. In all experiments, a best match rotation analysis was used to quantify the orientation, reliability, and coherence of the hippocampal map. First, for the analysis of the rectangular and isosceles triangular chambers, rate maps were compressed to squares and equilateral triangles, respectively, by using anisotropic pixels when generating the rate maps (short dimension 1 cm x long dimension 1.5 cm pixels for the rectangle; short dimension 1 cm x long dimension 1.42 cm for the triangle). Next, for each pair of trials (66 comparisons for 12 trials), the rotation of the Trial A rate map (square/rectangle: 0º, 90º, 180º, or 270º; triangle: 0º, 120º, 240º) that maximized the similarity to the Trial B rate map for each cell was computed. Similarity was calculated as the pixel-to-pixel cross-correlation between the two rate maps. To measure the likelihood of observing each orientation, the percent of pairwise trial comparisons for which each rotation yielded the best match was calculated for each cell. These proportions were then averaged within each animal as the orientations of simultaneously-recorded cells are likely not independent.

Rate map similarity. To measure the similarity of rate maps across trials for each cell, the best match rotation correlation value was computed for each pair of trial comparisons, and then averaged across all pairwise trial comparisons. This yielded a single correlation value for each cell indicating the similarity of that cell's rate maps across trials after aligning all trials. To test significance, the average correlation value across all cells was computed and compared to a shuffled control. This shuffled control was generated by randomly shuffling the rate maps across cells and trials prior to quantifying the rate map similarity using the same method (1000 iterations). The average correlation value across cells was then compared to the average correlation values from 1000 iterations of this shuffled control.

Orientation coherence. To measure the orientation coherence of simultaneously-recorded cell pairs, the patterns of best match rotations across all pairwise trial comparisons for both cells was compared. The similarity between these best match rotation patterns was quantified as the proportion of pairwise trial comparisons for which the same rotation yielded the best match. Trial comparisons for which at least one cell in the pair was inactive were excluded. To assess the significance of this orientation coherence, pattern similarity was compared to a shuffled control created by shuffling the best match rotation pattern for each cell independently. A cell pair was considered significantly coherent if its similarity exceeded the 99th percentile of 1000 iterations of this shuffled control. Note that this measure is sensitive to the distribution of best match rotations. Since two orientations tend to occur more often in the rectangular chamber, chance correspondences between the shuffled best match rotations are relatively common. Thus it is more difficult to distinguish true coherence from chance in the rectangular chamber than in the square chamber, where the even distribution of best match rotations yields fewer accidental co-occurrences following shuffling. This measure is also sensitive to the location of place fields. Specifically, the orientations of cells with fields near the center of the chamber are less clearly determined, and thus the best match rotations of these cells are inherently more variable. Because of these sensitivities, this measure sets a lower bound on orientation coherence.

Average behavior rate maps. Average rate maps corresponding to two behaviors (correct and geometric error searches) were created for each cell by concatenating the position and spiking activity vectors across all included trials. These data were then treated as a single trial and used to construct rate maps as described above.

Predicting Behavior. Behavior was predicted on the basis of population activity using a leave-one-out procedure. First, average behavior rate maps were created from correct and geometric error trials as described above, excluding the to-be-predicted trial. Then, the withheld trial rate maps were compared to the average correct and average geometric error rate maps by correlating the population vectors. The predicted behavior for the withheld trial was then the behavior corresponding to the average map with the higher population vector correlation. To assess whether the hippocampal map predicted search behavior prior to that behavior, we used two methods. First, we predicted search behavior on each trial using the same average map method, but only including data from incrementally longer time intervals (0 s to 60 s, in 0.5s steps) starting from the beginning of the to-be-predicted trial. Second, we predicted search behavior on each trial using the same average map method, but only including data prior to the first search during that to-be-predicted trial.

Bayes Factor. Bayes Factors were computed to verify that the hippocampal map was oriented by geometry and not nongeometric features [S5, S6]. When testing for an influence of geometry on best match rotations in the rectangular chamber, we compared the alternative hypothesis that the map was oriented by geometry (i.e., $p(0^o) + p(180^o) > 0.50$) to the null hypothesis that the map was not oriented by geometry (i.e., $p(0^o) + p(180^o) = 0.50$). When testing for an influence of the nongeometric features on best match rotations in the rectangular chamber, we compared the alternative hypothesis that the map orientation was anchored by the feature (i.e., $p(0^o) > p(180^o)$) to the null hypothesis that the map orientation was insensitive to the feature (i.e., $p(0^o) = p(180^o)$). When testing for an influence of the nongeometric feature on best match rotations in the square chamber, we compared the alternative hypothesis that the map orientation was anchored by the feature (i.e., $p(0^o) > 0.25$) to the null hypothesis that the map orientation was insensitive to the feature (i.e., $p(0^o) = 0.25$). When testing for stability of best match rotations in the triangular chamber, we compared the alternative hypothesis that the map was oriented by geometry (i.e., $p(0^o) > 0.33$) to the null hypothesis that the map orientation was insensitive geometry (i.e., $p(0^o) = 0.33$). To compute summary Bayes Factors for each test, the corresponding Bayes Factor was computed for each cell separately, averaged within animal, and then combined across animals to yield the final cumulative Bayes Factor.

Behavior Coding

Behavior during the spatial reorientation task was coded by two experimenters prior to the analysis of any electrophysiological data. The search behavior for each trial was defined as the first location in which the mouse dug for the reward. A dig was defined as an instance in which the mouse used one or both front paws to remove bedding from the medicine cup. Only when bedding was visible outside of the cup was a dig categorized as such. While digging behavior was typically very apparent, there was disagreement between raters on a subset (7/70, 10%) of trials. A tiebreaking rater was used to resolve the disagreement in these cases.

Histology

Electrode placement was verified after the completion of the experiments by passing a current (0.1mA for 5sec) through the tetrodes that yielded unit data (52500 Lesion Making Device, Ugo Basile). Then, mice were perfused with 10% formalin solution (Fisher Scientific). The brains were removed and fixed at 4ºC for at least 24hrs in 10% formalin containing 3% potassium ferrocyanide (J.T. Baker) for Prussian blue staining. Next, the brains were transferred to a 30% sucrose solution and kept for at least 24hrs at 4ºC for cryoprotection. The tissue was cryosectioned (30µm thick, coronal) and Nissl stained using standard histological procedures [S7].

Supplemental References

S1. Julian, J.B., Keinath, A.T., Muzzio, I.A., and Epstein, R.A. (2015). Place recognition and heading retrieval are mediated by dissociable cognitive systems in mice. Proc. Natl. Acad. Sci. *112*, 6503–6508.

S2. Kentros, C.G., Agnihotri, N.T., Streater, S., Hawkins, R.D., and Kandel, E.R. (2004). Increased attention to spatial context increases both place field stability and spatial memory. Neuron *42*, 283–95.

S3. Muzzio, I.A., Levita, L., Kulkarni, J., Monaco, J., Kentros, C., Stead, M., Abbott, L.F., and Kandel, E.R. (2009). Attention enhances the retrieval and stability of visuospatial and olfactory representations in the dorsal hippocampus. PLoS Biol. *7*, e1000140.

S4. Ranck, J.B. (1973). Studies on single neurons in dorsal hippocampal formation and septum in unrestrained rats. I. Behavioral correlates and firing repertoires. Exp. Neurol. *41*, 461–531.

S5. Gallistel, C.R. (2009). The importance of proving the null. Psychol. Rev. *116*, 439–453.

S6. Jeffreys, H. (1998). The theory of probability (Oxford: Oxford University Press).

S7. Powers, M.M., and Clark, G. (1955). An evaluation of cresyl echt violet acetate as a Nissl stain. Stain Technol. *30*, 83–8.